Author(s): Manderbacka, Teemu & Ruponen, Pekka & Kulovesi, Jakke & Matusiak, Jerzy

Title: Model experiments of the transient response to flooding of the box shaped barge

Year: 2015

Version: Post print

Please cite the original version:

Manderbacka, Teemu & Ruponen, Pekka & Kulovesi, Jakke & Matusiak, Jerzy. 2015. Model experiments of the transient response to flooding of the box shaped barge. Journal of Fluids and Structures. Volume 57. 127-143. ISSN 0889-9746 (printed). DOI: 10.1016/j.jfluidstructs.2015.06.002.

Model experiments of the transient response to flooding of the box shaped barge

T. Manderbacka[a,*], P. Ruponen[b], J. Kulovesi[c], J.E. Matusiak[a]

[a] *Aalto University, School of Engineering, Department of Applied Mechanics, Helsinki, Finland*
[b] *Napa Ltd, Helsinki, Finland*
[c] *Aalto University, School of Electrical Engineering, Department of Automation and Systems Technology, Helsinki, Finland*

Abstract

Coupling of the flooded water and ship motions was studied experimentally. Roll decay tests for one flooded compartment and transient abrupt flooding tests were performed for the box shaped barge model. The tests were conducted to obtain information on the flooding process for the development of numerical tools and to provide validation data. Quantitative values on the effect of flooded water on the roll damping were obtained. Flooded water behaves in a different manner in undivided and divided compartments. Flooded water in divided compartment increases roll damping significantly. In undivided compartment roll damping was high at low amount of flooded water. For higher amounts damping was of the same order as for the intact model. Initial flooding is a complex process where the ship and flooded water motions are coupled. Propagation of the flooding water inside the compartment, at a dam-break type abrupt flooding, was studied by tracking

*Corresponding author
Email address: teemu.manderbacka@aalto.fi (T. Manderbacka)

the surface of the flooded water. Image processing algorithm was used to obtain the tracked surface. Flooded water volume and its center of gravity were estimated from the tracked surface. Different internal layouts of the flooded compartment can lead to a totally different roll response. The inflooding jet plays an important role on the response in case of the undivided compartment. While, for a divided compartment, asymmetric flooding due to the obstructions, causes high heel angle on the damage side.
Keywords: sloshing, model tests, floodwater motion, floodwater progression, transient response

1. Introduction

The overall risk assessment of the marine traffic is dependent on the validity of underlying sub models (Goerlandt and Kujala, 2014; Ståhlberg et al., 2013). Collision between ships or grounding are the most common reasons for the loss of hull integrity and consequent flooding (Montewka et al., 2014). Understanding about the flooding process together with the ship response is one of the most important elements of existing risk models aiming at the improvement of the maritime traffic safety (Goerlandt et al., 2014). The flooding process can be divided into three stages; transient, progressive and steady state (Ruponen, 2007). The transient phase occurs right after the damage creation. Water starts to enter the ship through the damage opening. Inflow at this stage can be fast depending on the damage geometry. On the progressive stage the flooding continues through the internal openings of the ship. Transient and progressive stages are often referred to as the intermediate stages of flooding. At these stages the flooding

process is complex depending, among many factors, on hydrostatical and geometrical characteristics of the ship (Khaddaj-Mallat et al., 2011). A large passenger vessel may lose its stability during the transient and intermediate stages of flooding (Vassalos et al., 2004).

The intermediate stages of the flooding include the impact of the inflow momentum and the flow propagation inside the compartment (Journée et al., 1997). Ship motions, floodwater movements and the progression of the flooding are strongly coupled. Asymmetric flooding due to obstructions in the compartment can cause a significantly high transient roll on the damage side or even capsize at the initial stage (Spouge, 1985; Vredeveldt and Journée, 1991; Santos et al., 2002; Macfarlane et al., 2010). For a compartment free of obstructions a jet due to the inflooding pushes the water to the opposite side and roll angles to the opposite side of the damage are observed in the model tests (Ikeda and Ma, 2000; de Kat and van't Veer, 2001; Ikeda and Kamo, 2001; Ikeda et al., 2003). Roll motion to the opposite side of the damage can slow down the inflooding by lifting the opening above the sea surface (Ikeda and Ma, 2000). The ship may experience a high roll angle either on the damage or on the opposite side depending on the initial water motions in the flooded compartment.

The coupling of the ship motions and liquid sloshing has been studied in the context of liquid transportation (Journée, 1997; Faltinsen and Timokha, 2009) specially related to the LNG tanks (Zhao et al., 2014). Essential differences, in the case of the damaged ship compared with the sloshing in liquid transportation, are the changing amount of water in the compartment and often lower fill height per tank breadth ratio at all stages of flooding.

Intact and damaged ship motion response in waves have been studied by Armenio et al. (1996a,b), Chan et al. (2002), Korkut et al. (2004) and Begovic et al. (2013). They observed smaller roll motion response for the damaged ship than for the intact ship. In a numerical and experimental study of the damage ship motions in waves by Lee et al. (2007) it was concluded that more investigation is needed on the flooded water motions and progression inside the compartments. Free roll decay tests of the damaged ship (de Kat, 2000; Papanikolaou, 2001; Papanikolaou and Spanos, 2004; Lee et al., 2012) have showed that flooded water increases both damping and the period of the roll motion. In the previous studies the complex coupled flooded water motions have been observed to cause nonharmonic and damped roll response. Bouscasse et al. (2014a,b) performed experimental and theoretical study on the energy dissipation due to water motions. The internal layout of the damaged compartment has an important effect on the flooded water progression and motions (van't Veer and de Kat, 2000; van't Veer et al., 2004; Khaddaj-Mallat et al., 2012). Water exchange between the compartments through non-watertight openings in a harmonic motion of the compartment has been studied by Manderbacka et al. (2014). The beginning of the flooding resembles a dam-breaking problem which has been widely studied both numerically and experimentally (Lobovský et al., 2014). However, the damaged ship response complicates the problem.

The aim of this study is to provide quantitative data on the damping and flooded water motions in the damaged ship. In this paper a thorough set of measurements on simplified ship geometry is presented. Model proportions of external/internal dimensions, stability and inertia properties are relevant

to a real ship. Coupling of the ship roll response to the water motions is studied by performing roll decay tests for flooded ship. The inflooding process at the initial stages of the flooding is carefully studied by transient flooding tests. Inflooding water kinematics is studied by tracking the water surface and estimating the flooded water volume and location of its center of gravity. This information is of utmost importance when validating the computational tools. The effect of the compartment layout and initial stability have been studied by performing tests with two different compartments and two different initial stabilities. Air flow and compression may further complicate the flooding process (Palazzi and de Kat, 2004; Ruponen et al., 2013). In this study the air compression effect is eliminated by having all flooded spaces fully ventilated . The geometry of the compartment layout had been made as simple as possible in order to concentrate and reveal the importance of different phenomena in flooding case. The simplified geometry facilitates comparison to computational models for validation purposes. The measurements reveal the importance of the flooded water motions on the response of the model.

This paper adds to the existing literature by providing systematic study on the damping effect of the flooded water. Furthermore quantitative data of the water motions at transient stage was obtained. Small values of flooded water can dampen the roll very fast if the sloshing natural frequency is close to the ship natural roll frequency. In this case the flooded water acts like a passive anti-rolling tank. Flooded water in the compartment with obstructions dampens the roll motion very efficiently. For the compartment with obstructions the increase in the amount of flooded water increases the damp-

ing. In the undivided compartment the inflooding water jet pushes the water to the opposite side of the damage and causes roll to that side. The amount of flooded water and its position have been obtained by tracking the surface of flooded water using the video recordings.

In section 2 first a general description of the experiment arrangements is given. Then the model geometry and instrumentation are described in subsection 2.1 and subsection 2.2, respectively. Followed by the subsection 2.3 and subsection 2.4 where the experimental campaign is represented. The ship response and flooded water heights are shown in the measurement results section 3. The process of water ingress is studied. Finally, the obtained results are discussed in section 4 and the main conclusion are given in section 5.

2. Experiment arrangement and methods

Model tests were performed at Aalto University towing tank. The tank is 130 m long, 11 m wide and 5.5 m deep. Water density in the tank was $\rho = 1000$ kg/m^3 and gravitational acceleration $g = 9.819$ m/s^2 (provided by MIKES Centre of Metrology and Accreditation for tank location). Experiments were performed for the box shaped barge model (Figure 1). This same model was used for progressive flooding tests performed at Aalto University (former Helsinki University of Technology) (Ruponen, 2006; Ruponen et al., 2007) and it is used for the ITTC benchmark study (van Walree and Papanikolaou, 2007). In this study the load case and opening arrangement were changed in comparison to the previous tests. Length of the model is 4 m, other main particulars are given in Table 1. Proportions of the model's main dimensions are similar to a typical passenger ship. Length per breadth ratio

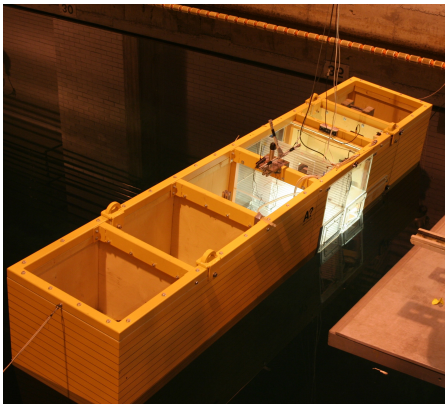

(a) Model in tank.

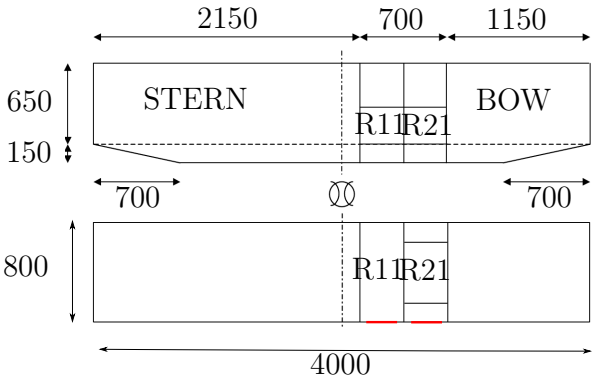

(b) Overall dimensions of the model and compartment locations (Ruponen, 2006).

Figure 1: Box-shaped-barge model.

$L/B = 5$ and breadth per draft ratio $B/T \approx 3.16$. Model was adjusted to two different initial stabilities $\overline{GM}_{0,1}/B \approx 0.024$ and $\overline{GM}_{0,2}/B \approx 0.034$. Roll radius of gyration per ship breadth $r_{xx}/B \approx 0.4$. Nominal scale of 1:40 would result in a full scale ship of length 160 m and initial stabilities of $\overline{GM}_{0,1FS} \approx 0.8$ m and $\overline{GM}_{0,2FS} \approx 1.1$ m. The length per breadth ratio and the initial stability of the model are somewhat smaller than than for a typical passenger ship Levander (2003-2004).

One compartment flooding was tested. Roll decay in flooded condition and transient flooding tests were performed for freely floating barge model in calm water. The model was positioned transversally in the middle of the tank. This way diffractions from the tank walls of waves radiated by the model roll motion were minimized. The model was moored to the tank sides from the stern and bow with slack elastic strings. They provided minimal mooring force. Sway motion period due to the mooring was more than two

Table 1: Intact barge main particulars for two different initial metacentric heights.

	$\overline{GM}_{0,1}$	$\overline{GM}_{0,2}$	precision
Length, L	4.000 m		0.005 m
Breadth, B	0.800 m		0.002 m
Draft, T	0.253 m		0.001 m
Total mass, m	657 kg		1.0 kg
Vertical center of buoyancy, $\overline{KB}_0$	0.144 m		
Metacentric height from keel, $\overline{KM}_0$	0.404 m		
Initial metacentric height, $\overline{GM}_0$	0.0189 m	0.0274 m	0.0008 m
CoG height from keel, $\overline{KG}_0$	0.385 m	0.377 m	
Natural roll period, T_ϕ	5.49 s	4.50 s	0.0024 s
Roll damping ratio, ξ	0.036	0.025	0.0023
Roll moment of inertia, I_{xx}	80.9 kg m^2	79.2 kg m^2	

minutes, which is more than decade higher than the maximum measured roll periods. Thus the mooring effect on the model motions is considered negligible.

Roll decay in flooded condition was tested for flooded water weights ranging from 0.38 % to 3.8 % of the intact model displacement. In the transient flooding tests a damage opening with the length of 5 % of the model length was introduced onto the side hull of the model. Damage opening length is nearly 60 % of the compartment length.

2.1. Barge model

Barge hull geometry is symmetric with respect to the midship. The barge model has vertical sides and rectangular water plane area (Figure 1). The main particulars are given in Table 1. The model is constructed of wooden stern and bow sections and a of an acrylic glass compartment section. The stern and bow sections are mounted together with an upper steel frame visible in Figure 1a. On the bottom the sections are connected by two aluminium T-beams acting as bilge keels. Total height of the T-beam is 60 mm, web and flange thickness is 5 mm. The compartment section is a cassette like structure inserted between the stern and bow sections. Detailed description of the model construction is given in Ruponen (2006) and the supplementary data including hull geometry can be found in Napa Ltd and Aalto University (2013). Dimensions of the sections are given in Figure 1b.

Compartments R11 and R21 are located on the bow side of the model. Both compartments are of the same size. Compartment R11 is clear of all obstructions while compartment R21 has two non-watertight longitudinal bulkheads (Figure 2). Compartments are referred to as undivided R11 and

divided compartment R21. The only openings inside the barge are the openings on the bulkheads between the rooms R21S, R21 and R21P. They are chamfered so that the openings have one sharp 90 degrees edge. Two openings inside compartment R21 are 20 mm wide and 200 mm high.

The outer hull damage opening was separately introduced to the compartments R11 and R21. It is a rectangular 200 mm $\times$ 200 mm size opening on the starboard side. Corners of the damage opening have 12 mm rounding. Wall thickness is 10 mm. Damage opening walls do not have any chamfer or rounding. Initial tank water level was 38 mm above the damage opening.

2.2. Measurement setup

The barge position with respect to the inertial frame was measured optically. Water heights in the compartment were measured with wave probes. In the damage opening tests, the hatch opening instant was recorded. Position and water height measurement systems were connected to the same data logger together with the damage opening circuit. Data was logged at sampling rate 127 samples per second.

The barge position was measured with an optical measurement system consisting of a Krypton Rodym camera-target system and CTrack software. The barge was equipped with a target, which consists of three led lights (Figure 1a). The camera records the positions of the led lights and the software outputs the position and angular orientation of the target i.e. the barge with respect to the inertial coordinate frame, where Z is positive downwards and ϕ positive for roll on starboard. The center point of the target is located at the midship at height 1028 mm from the bottom. Target height above the intact barge water line $h_t = 775$ mm.

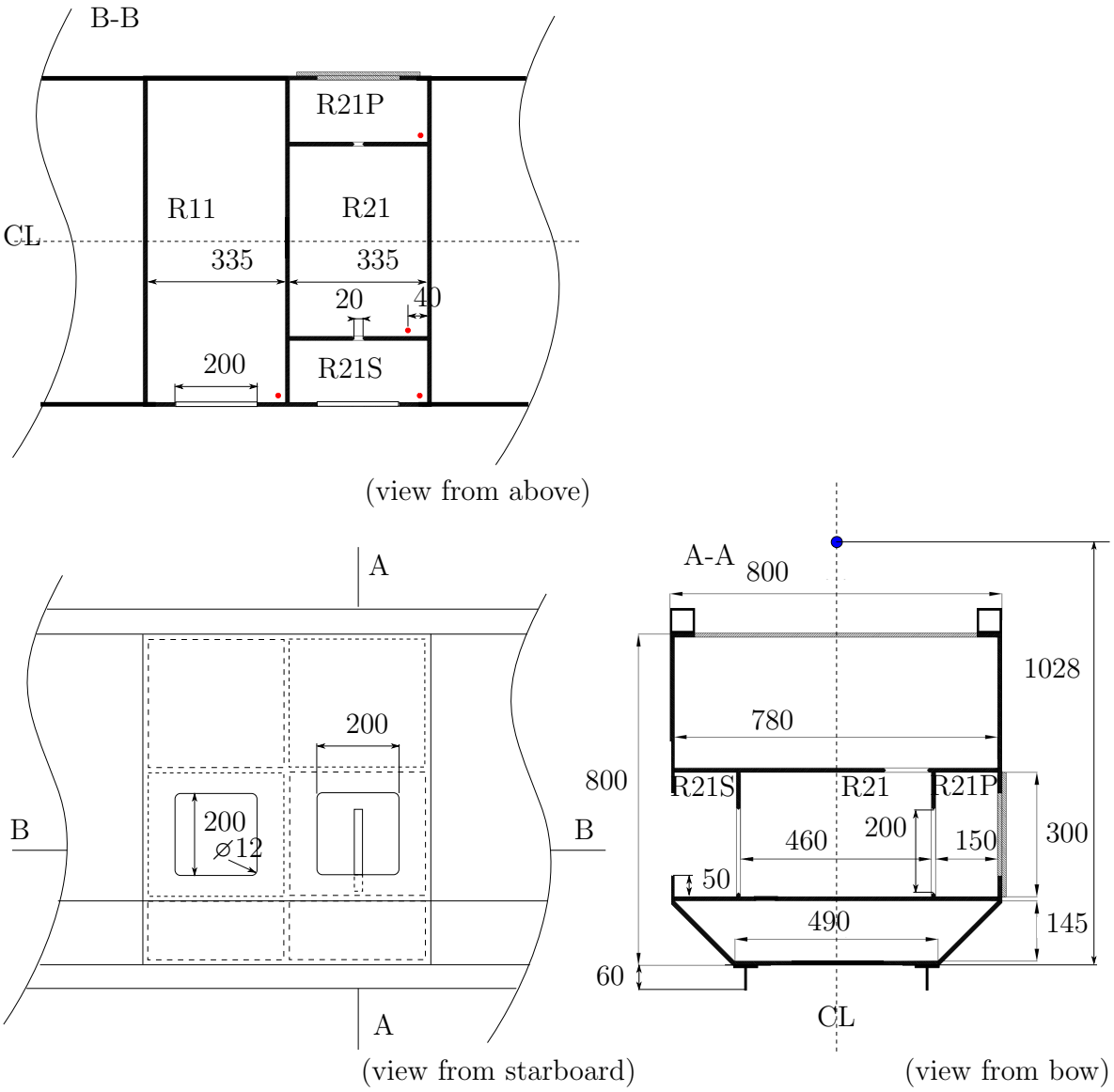

Figure 2: Dimensions of the compartments and openings. Positions of the water height sensors are marked with red dots. Position of the target center point is marked with blue dot.

The measured vertical position is expressed as the increase in draft Z. The increase in the draft is the change in the vertical position of a point at intersection between the barge center line and the intact barge water line. Increase in draft is calculated from the measured position

$$Z = Z_t - h_t(1 - \cos(\phi)\cos(\theta)) \ , \tag{1}$$

where Z_t is the vertical position of the target center point, ϕ is the measured barge roll angle and θ is the measured trim angle.

Precision of the angle and position measurement are estimated to be $\phi_e = 0.2$ deg and $Z_{t,e} = 0.5$ mm respectively. Height of the target is estimated to be measured at accuracy of $h_{t,e} = 0.5$ mm. The total error in the Z coordinate can then be estimated as

$$\begin{aligned} Z_e &= \phi_e \left|\frac{\partial Z}{\partial \phi}\right| + \theta_e \left|\frac{\partial Z}{\partial \theta}\right| + Z_{m,e}\left|\frac{\partial Z}{\partial Z_m}\right| + h_{t,e}\left|\frac{\partial Z}{\partial Z_t}\right| \\ &= \phi_e h_t \sin(\phi)\cos(\theta) + \phi_e h_t \cos(\phi)\sin(\theta) \\ &\quad + Z_{m,e} + h_{t,e}(1 - \cos(\phi)\cos(\theta)) \ . \end{aligned} \tag{2}$$

At given estimated accuracies applying the above equation $Z_e \approx 1.0$ mm at roll angle of 10 deg and at zero trim angle.

Water heights in in the compartments were measured with resistance type wire pair probes. The wire diameter is 2 mm and the distance between the wires pair centers in one probe is 7.5 mm. Water height probes are located close to the corner of each flooded space, R11, R21, R21S and R21P, (Figure 2). Distance of the water height probe from the vertical walls is approximately 5 mm, except in room R21, where the distance from the transversal bulkhead is 40 mm.

Inflooding at the transient flooding tests were video recorded by a GoPro camera model HERO2, which was placed in the adjacent compartment viewing the flooded compartment through the transversal acrylic glass bulkhead. Recording was performed at speed of 60 frames per second. Frames were not interlaced. Resolution was 1280 $\times$ 720 pixels. Video frames were cropped to present the flooded area of the compartment. At transient flooding tests for compartment R11 the effective area is 672 $\times$ 165 pixels. A quantitative value for the water motion is derived from the video recordings. The surface elevation on the back wall of the compartment is tracked for each frame using the video processing algorithm adapted from methods described in Manderbacka et al. (2014). The tracking method is based on global image intensity difference thresholding. The surface is assumed to remain two dimensional i.e. the water elevation in the compartment is assumed not to vary in the longitudinal direction of the barge. Synchronization between the video recordings and initiation of the damage opening was achieved with a led light, which indicated the initiation of the damage opening. Led light was connected to the damage opening trigger system. When the trigger was released, it cut the led circuit and thus the light. All the transient flooding measurements were synchronized to the damage opening initiation with the help of the led circuit channel signal.

2.3. Preparative tests

2.3.1. Intact model

Initial properties for the intact model were defined by the inclining test, roll inertia measurement and roll decay test. These properties for both initial stabilities are listed in Table 1.

The initial stability of the model i.e. the metacentric height $\overline{GM}_0$ was measured with inclining tests. The inclining test is based on the approximation of initial stability, which requires small heel angles. The heeling moment caused by the mass m_w is $M_{heel} = m_w g e_w \cos\phi$, where e_w is the distance between center line and heeling weight. The static righting moment is $M_{st} = -mg\overline{GM}_0 \sin\phi$, where m is the mass of the barge model. In the equilibrium condition $M_{heel} + M_{st} = 0$, which gives a formula for the initial metacentric height

$$\overline{GM}_0 = \frac{m_w e_w}{m \tan\phi} \, . \tag{3}$$

The inclining test was performed by moving a mass of $m_w = 4.915$ kg, pertaining to the model, in the transversal direction and measuring the heel angle. Ten measurement points at angles less than six degrees were taken.

Precision of definition of initial stability can be estimated from the accuracy of the mass used to provide the heeling moment $m_{w,e} = 0.005$ kg, measurement of the transversal position of the mass $e_{w,e} = 0.001$ m, barge model total mass $m_e = 1.0$ kg and accuracy of the angle measurement $\phi_e = 0.2$ deg

$$\begin{aligned} \overline{GM}_{0,e} &= m_{w,e}\left|\frac{\partial \overline{GM}_0}{\partial m_w}\right| + e_{w,e}\left|\frac{\partial \overline{GM}_0}{\partial e_w}\right| + m_e\left|\frac{\partial \overline{GM}_0}{\partial m}\right| + \phi_e\left|\frac{\partial \overline{GM}_0}{\partial \phi}\right| \\ &= m_{w,e}\left|\frac{e_w}{m\tan\phi}\right| + e_{w,e}\left|\frac{m_w}{m\tan\phi}\right| + m_e\left|\frac{m_w e_w}{m^2\tan\phi}\right| + \phi_e\left|\frac{m_w e_w}{m\sin^2\phi}\right| \, . \end{aligned} \tag{4}$$

The total precision of the initial stability is estimated to be $\overline{GM}_{0,e} = 0.8$ mm with the accuracies mentioned above and at heel angle 5.7 degrees in the Equation 4.

Roll decay tests were initiated with an approximately five degrees heel angle. Roll motion is assumed to have first order linear damping according

to the linear roll equation of motion

$$\ddot{\phi} + 2\xi\omega_\phi\dot{\phi} + \omega_\phi^2\phi \ . \tag{5}$$

Natural roll period $T_\phi = \frac{2\pi}{\omega_\phi}$ and roll damping factor ξ were defined by fitting the solution

$$\phi(t) = \phi_0 \ e^{-\xi \ \frac{2\pi}{T_\phi} \ t} \ \cos\left(t\frac{2\pi}{T_\phi}\sqrt{1-\xi^2}\right) \tag{6}$$

of the roll equation of motion to the measurement time histories of the roll decay tests for the intact model.

2.3.2. Discharge coefficients

The discharge coefficient C_d of the damage opening was evaluated. This was done by measuring the free discharge from compartment R11 into the air. The water height H in the compartment was measured. For a tall opening the pressure on the height of the opening varies. Flow rate Q through the tall opening is governed by the following equation derived from the Bernoulli equation (Ruponen, 2007)

$$Q = C_d l_o \frac{2}{3}\sqrt{2g}\,(H - H_{min})^{3/2} \ , \tag{7}$$

where $l_o = 200$ mm is the horizontal length of the opening and $H_{min} = 50$ mm is the height of the lower edge of the opening from the bottom of the compartment. Volume of water V in the compartment is expressed with the water height and compartment bottom area $S = 0.2613$ m^2, ($V = H \ S$). Equation for the volume change in the compartment

$$\begin{aligned} \frac{dV}{dt} &= -Q \\ \frac{dH}{dt}S &= -C_d l_o \frac{2}{3}\sqrt{2g}\,(H - H_{min})^{3/2} \end{aligned} \tag{8}$$

is then integrated from the initial water height H_0 at $t = 0$ to the water height $H(t)$

$$\int_{H_0}^{H(t)} dH = -\int_0^t \frac{2C_d l_o}{3S}\sqrt{2g}\,(H - H_{min})^{3/2}\,dt \tag{9}$$

and the equation for the instantaneous water height is obtained

$$H(t) = H_{min} + \frac{H_0 - H_{min}}{\left(\frac{1}{3S}C_d l_o \sqrt{2g(H_0 - H_{min})}\; t + 1\right)^2}\ , \tag{10}$$

where H_0 is the initial water height.

2.4. Test sequences

Sets of test cases were planned in increasing complexity. Discharge coefficients for the openings were evaluated by discharging the water from the compartment to the air when the model was set stationary out of water. Then two sets of the roll decay test were first performed for the intact barge model at both initial stabilities. After that the roll decay tests were performed for the barge model with different amounts of water in the compartment R11 and R21 separately. Again at both initial stabilities. Finally tests for the initiation of the damage opening were performed. The damage initiation tests were separately performed for the damage into compartment R11 and R21. All the tests were performed for two different initial stabilities $\overline{GM}_{0,1}$ and $\overline{GM}_{0,2}$.

2.4.1. Roll decay tests for flooded ship

During the flooding process the ship experiences roll motions at different amounts of flooded water. In order to provide data on the coupling of the ship and flooded water motions, roll decay tests with constant amount of

water were performed. The amounts of the water with which the roll decay was tested ranged from very low fill height to the amount close to the final equilibrium state at the damage opening case. The damage opening was kept closed in the roll decay test so no water exchange to or from the sea took place. Damage opening was closed with a plate that was placed on the external surface of the model (Figure 5). Water inside the compartment was able to occupy the actual damage opening shown in Figure 2. For this reason the compartment is not totally symmetrical. In compartment R21 the internal openings in the longitudinal bulkheads were open.

Natural sloshing periods are dependent on the water height and tank breadth. Ship motions at period close to the natural sloshing period excite the sloshing. The lowest natural frequency ω_0 of the lateral water sloshing in a rectangular compartment with breadth b can be estimated with the linear potential theory for water height h (Lamb, 1945)

$$\omega_0^2 = \frac{g\pi}{b} \tanh\left(\frac{\pi h}{b}\right) \ . \tag{11}$$

The natural sloshing periods T_0 are estimated by the linear potential theory for each fill ratio at different amounts of water m in the compartment. Fill ratio in Table 2 is the average water depth in the compartment h per room breadth, $b = 780$ mm for R11 undivided compartment breadth, $b_S = 150$ mm for the side rooms R21S and R21P and $b_M = 460$ mm for the middle room of the compartment R21.

Roll decay was tested for compartments R11 and R21 at two different initial metacentric heights $\overline{GM}_{0,1}$ and $\overline{GM}_{0,2}$. Model GZ curve for different amount of water was calculated numerically with NAPA software applying the added weight method. Actual geometry accounting for the internal and

Table 2: Mass of the water m and the natural sloshing periods estimated by potential theory.

		R11		R21S, R21P		R21	
case	m(kg)	h/b_{R11}	T_0(s)	h/b_S	$T_{0,S}$(s)	h/b_M	$T_{0,M}$(s)
D1	2.5	0.012	5.09	0.065	0.97	0.021	2.97
D2	5.0	0.025	3.60	0.131	0.70	0.043	2.10
D3	10.0	0.049	2.56	0.262	0.53	0.085	1.50
D4	15.0	0.074	2.10	0.393	0.48	0.128	1.24
D5	20.0	0.098	1.83	0.524	0.45	0.171	1.10
D6	25.0	0.123	1.65	0.655	0.45	0.213	1.00

damage opening was modelled. Restoring moment for the lower initial stability $\overline{GM}_{0,1}$ (Figure 3) is close to zero at smaller angles for all the amounts of the water in the compartment. The loll angle to which the barge sets at these flooded water amounts is a few degrees. The restoring moment is positive at high heel angles due to high vertical free-board of the model. For higher initial stability $\overline{GM}_{0,2}$ (Figure 4) the loll angle is close to zero, but not exactly zero due to the damage opening making the space non-symmetrical. Calculated trim angles at the highest amount of flooded water 25.0 kg in compartment R11 are 0.11 deg at both initial stabilities. The calculated trim angle at the same amount of water 25.0 kg in compartment R21 are 0.23 deg at both initial stabilities.

Before the tests the water to be added into the compartment was weighted with a scale, which had accuracy of 0.005 kg. The experiments of the roll de-

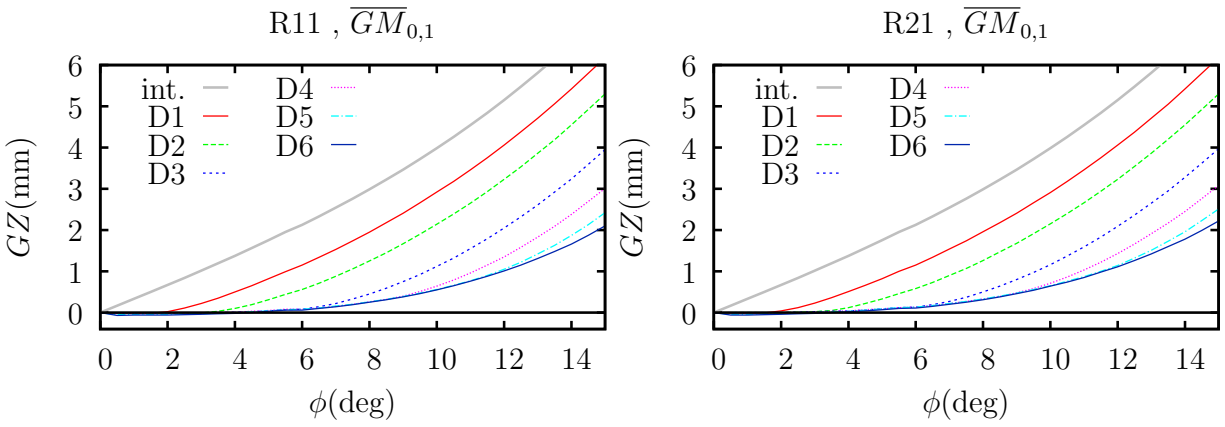

Figure 3: GZ curves for intact model and for different water amounts at lower initial stability calculated with NAPA.

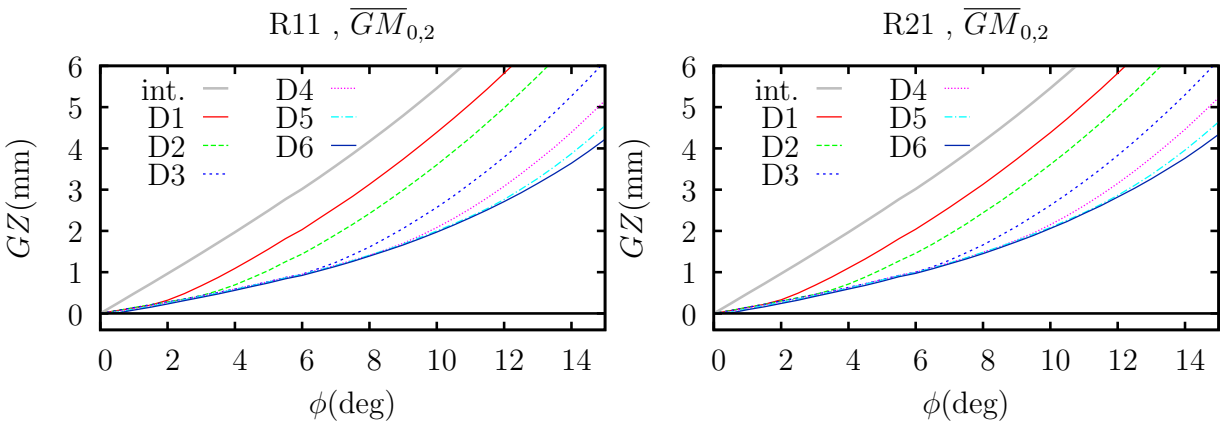

Figure 4: GZ curves for intact model and for different water amounts at higher initial stability calculated with NAPA.

cay for constant amount of water in the damaged compartment were initiated with the same heeling load on the side of the barge for all tests. The heeling load was introduced to the barge model with a 5 kg weight positioned on the starboard side of the upper frame of the model at midship. The weight was removed by lifting it with a non-elastic cord attached to it, so that the contact between the model and weight was lost immediately. The friction between the weight and the model is believed to be negligible, thus the influence of the weight on the model is assumed to be removed immediately when the weight is lifted. As the load was removed, the model was allowed to roll and decay freely. The initial heel angle is different for all the tests due to different water amounts and thus different total restoring moment. The final equilibrium position differs from the even keel position.

The roll damping ratio for roll decay tests with constant amount of water was estimated by fitting an exponential decay curve to the half range peak to peak roll angles. The curve fitted was

$$f(t) = \phi_0 \; e^{-\xi \; \omega_0 \; t} \; , \tag{12}$$

where ϕ_0 and ξ are constants estimated by the linear least square error fitting. The natural roll frequency ω_0 for the intact barge was applied. The restoring moment, as shown in Figure 3 and 4 in a form of GZ curves, is nonlinear. Thus the linear roll equation model is not very well suited for this case. The exponential decay curve is applied in order to obtain an estimate for the damping. The time between the roll peak to peak values was also calculated. The time from peak to peak is multiplied by two in order to be comparable to the roll period.

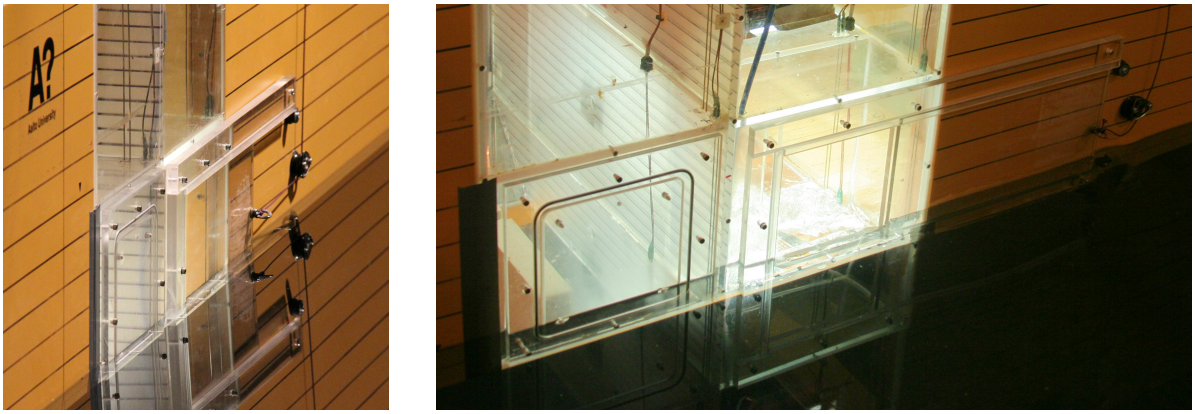

(a) Closed. (b) Open.

Figure 5: Damage opening mechanism. Setup for the damage to compartment R21.

2.4.2. Transient flooding tests

Compartments R11 and R21 were flooded separately during the tests. The damage opening was closed by a plate before the test. The plate was pulled aftwards for the damage to compartment R11 and forwards for damage to compartment R21 by a string connected to a tensioned spring to initiate the inflooding (Figure 5a). The tensioned spring was held by a trigger, which was released actuating a radio controlled servo motor. The sliding plate closing the damage opening was sealed by applying silicone grease between the plate and external hull around the opening in order to ensure water tightness. From the video recordings hatch opening time was estimated to be approximately 0.1 s or faster.

3. Results

3.1. Preparative test

3.1.1. Discharge coefficients

Discharge coefficient for the damage opening was found by fitting Equation 10 to the measured water height time history in the compartment R11. Discharge was measured with three different initial water heights $H_{0,1} = 90$ mm, $H_{0,2} = 142$ mm and $H_{0,3} = 104$ mm. Some sloshing can be observed in the measured water heights in Figure 6. The opening is relatively large, nearly 60 % of the compartment length. When the hatch is opened the water height on the opening side of the compartment, where the height probe is located, drops faster causing sloshing in the compartment. Discharge coefficients at different initial water heights $H_{0,1}$, $H_{0,2}$ and $H_{0,3}$ were found to be $C_{d,1} \approx 0.682$, $C_{d,2} \approx 0.635$ and $C_{d,3} \approx 0.646$, respectively. Discharge coefficients for the openings inside the compartment R21 were evaluated by Ruponen (2006). Measurements were repeated three times. The average values and standard deviations of the evaluated discharge coefficients are listed in Table 3. Standard deviation of the damage opening discharge coefficient is bigger than for the inside opening. The sloshing during the experiment reduces the accuracy of estimation of the discharge coefficient because the horizontal water plane was assumed for Equation 10.

3.1.2. Intact model

Values of initial metacentric height $\overline{GM}_0$ are evaluated by fitting Equation 3 to the results plotted in Figure 7. Obtained metacentric heights are $\overline{GM}_{0,1} = 0.0189$ m and $\overline{GM}_{0,2} = 0.0274$ m. For the lower initial stability

Table 3: Discharge coefficients. Data for opening inside R21 from Ruponen (2006).

Opening	Size	Average C_d	Standard deviation
Inside R21	20 × 200	0.75	0.0096
Damage opening	200 × 200	0.65	0.0244

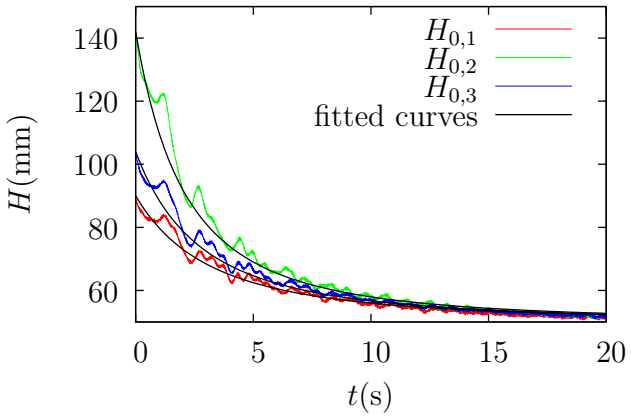

Figure 6: Water height in the compartment R11 for free discharge into air, measurements at initial heights $H_{0,1}$, $H_{0,2}$ and $H_{0,3}$. Fitted curves for initial heights with $C_{d,ext} = 0.654$

.

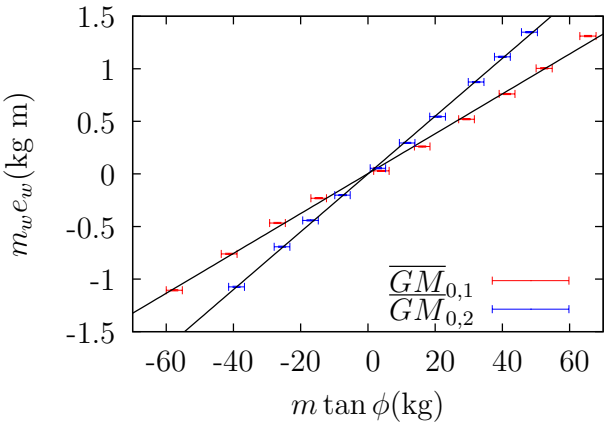

Figure 7: Results of the inclining test for both initial stabilities and fitted curve at defined initial stability.

$\overline{GM}_{0,1}$ roll decay test was repeated 5 times (Figure 8a). Natural roll period and the damping ratio were found by fitting Equation 6 to the measurement time histories. The average value of the roll natural period for the lower initial stability was 5.494 s with the standard deviation of 0.0024 s and roll damping ratio 0.036 with the standard deviation of 0.0023. Repeatability of the roll decay test for the intact model was found to be good and for higher initial stability $\overline{GM}_{0,2}$ the test was repeated only 3 times (Figure 8b). The average value of roll natural period for higher initial stability was found to be 4.502 s with the standard deviation 0.0015 s and natural damping ratio 0.025 with the standard deviation of 0.0019.

3.2. Roll decay tests for flooded ship

Time histories of measured roll angle for the roll decay tests with constant amount of flooded water in compartments R11 and R21 are presented in Figure 9. Roll time history for flooded compartment R11 with low initial

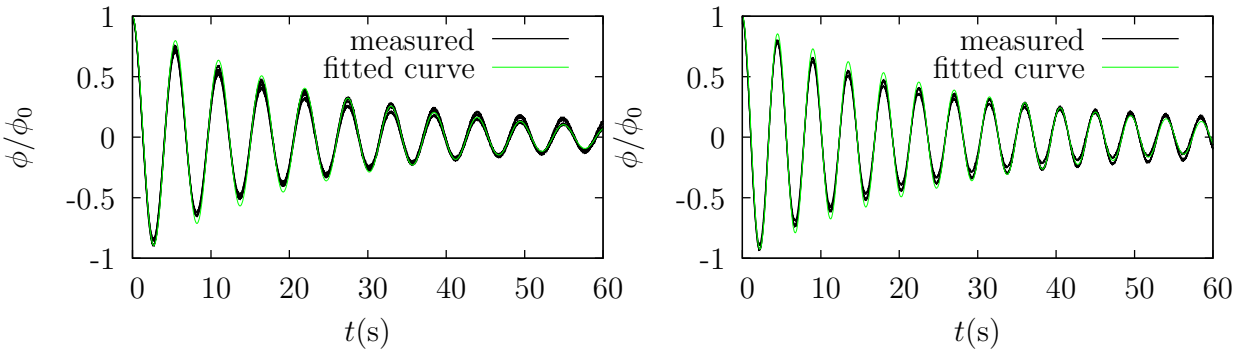

(a) $\overline{GM}_{0,1}$ (b) $\overline{GM}_{0,2}$

Figure 8: Roll decay test for intact model.

stability $\overline{GM}_{0,1}$ changes significantly at different water amounts. The periods of the roll motions vary from period to another. It can be observed that the roll is non-harmonic with a varying and decaying amplitude, Figure 9a. At higher initial stability $\overline{GM}_{0,2}$ for compartment R11 roll time histories behave in a more harmonic nature. The length of the periods seems to be affected by the amount of the water and within each test they seem not to change much. The roll decay seems to be faster for smaller water amounts, Figure 9b. For the roll decay tests with constant amount of water in the compartment R21 (Figure 9c and 9d) the roll time histories behave in a more harmonic nature than for the compartment R11. The period of the roll is not much affected by the amount of water. Roll motion decays faster for bigger amounts of water, conversely to the roll decay tests with compartment R11.

The above mentioned observations from the presented roll time histories are studied more in detail by the peak values of the roll angle, Figure 10. The local minima and maxima of each roll time history are identified and the

stroke from peak to peak is then calculated and divided by two to present a sort of an envelope curve around the mean roll angle in time. The halved peak to peak values show the decay of the roll. The roll decay is slower for the compartment R11 (Figure 10a and 10b) than for the compartment R21 (Figure 10c and 10d) except for the case with the smallest amount of water.

The intact ship roll period is marked in the figures together with the peak to peak periods. Peak to peak periods for roll amplitudes smaller than 0.5 degree are disregarded in the analysis. For the compartment R11 the half periods experience some variations in the beginning of the tests with lower initial stability (Figure 10a). At higher initial stability the roll periods have nearly constant values and are close to double the natural roll period of the intact barge (Figure 10b). In the measurements for compartment R21 the roll periods are close to the intact barge natural roll period (Figure 10c and 10d).

Estimated roll damping ratios are plotted in Figure 11 for both tested compartments and both initial stabilities as a function of water mass in the compartment. Roll damping for undivided compartment R11 is the highest at the lowest fill amount and decreases as the amount of the water is increased. For the divided compartment R21 the behaviour is the opposite. The roll damping is increased by increasing the amount of water in the divided compartment.

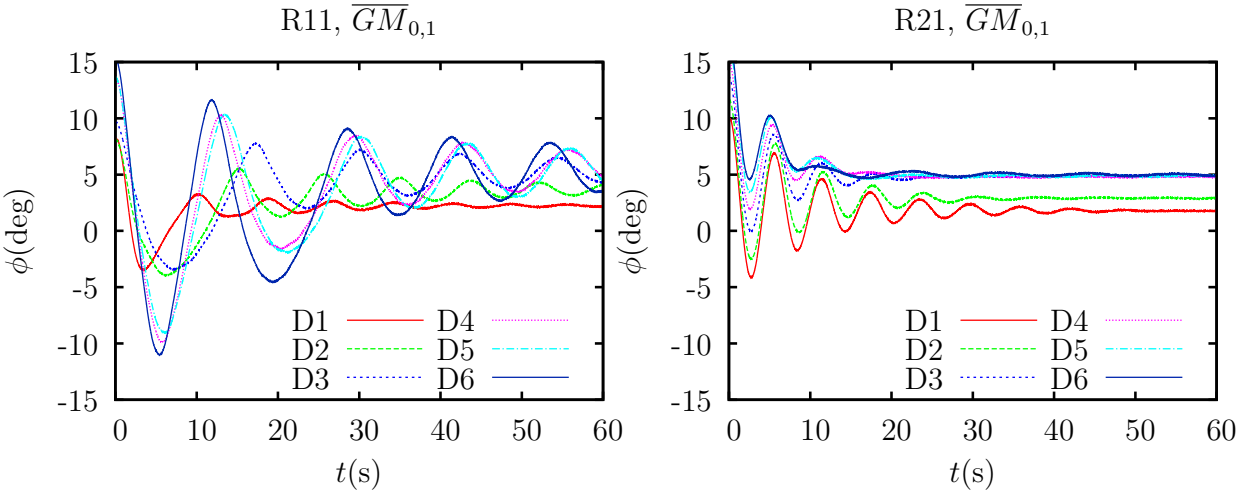

(a) Compartment R11. Lower initial stability $\overline{GM}_{0,1}$.

(c) Compartment R21. Lower initial stability $\overline{GM}_{0,1}$.

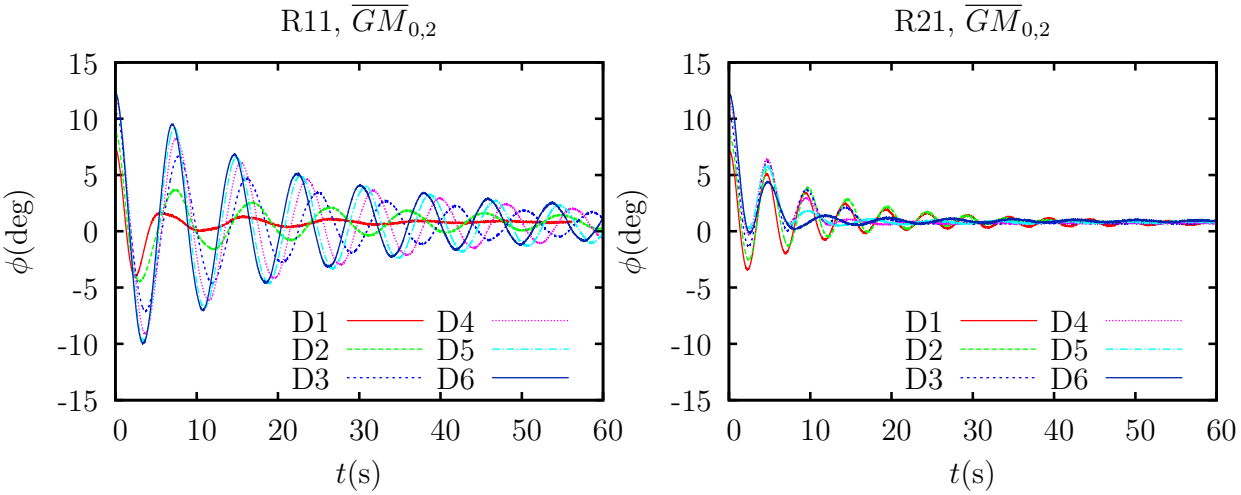

(b) Compartment R11. Higher initial stability $\overline{GM}_{0,2}$.

(d) Compartment R21. Higher initial stability $\overline{GM}_{0,2}$.

Figure 9: Roll angle, roll decay tests with constant amount of flooded water in compartment

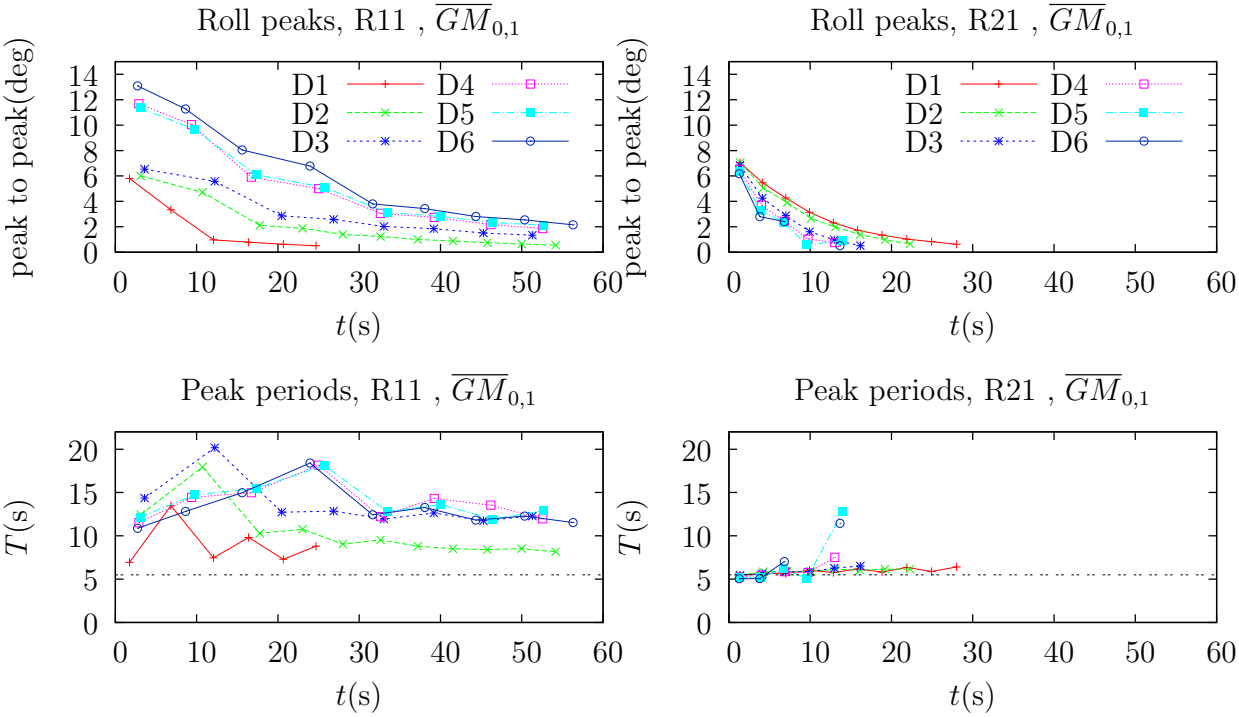

(a) Compartment R11. Lower initial stability $\overline{GM}_{0,1}$.

(c) Compartment R21. Lower initial stability $\overline{GM}_{0,1}$.

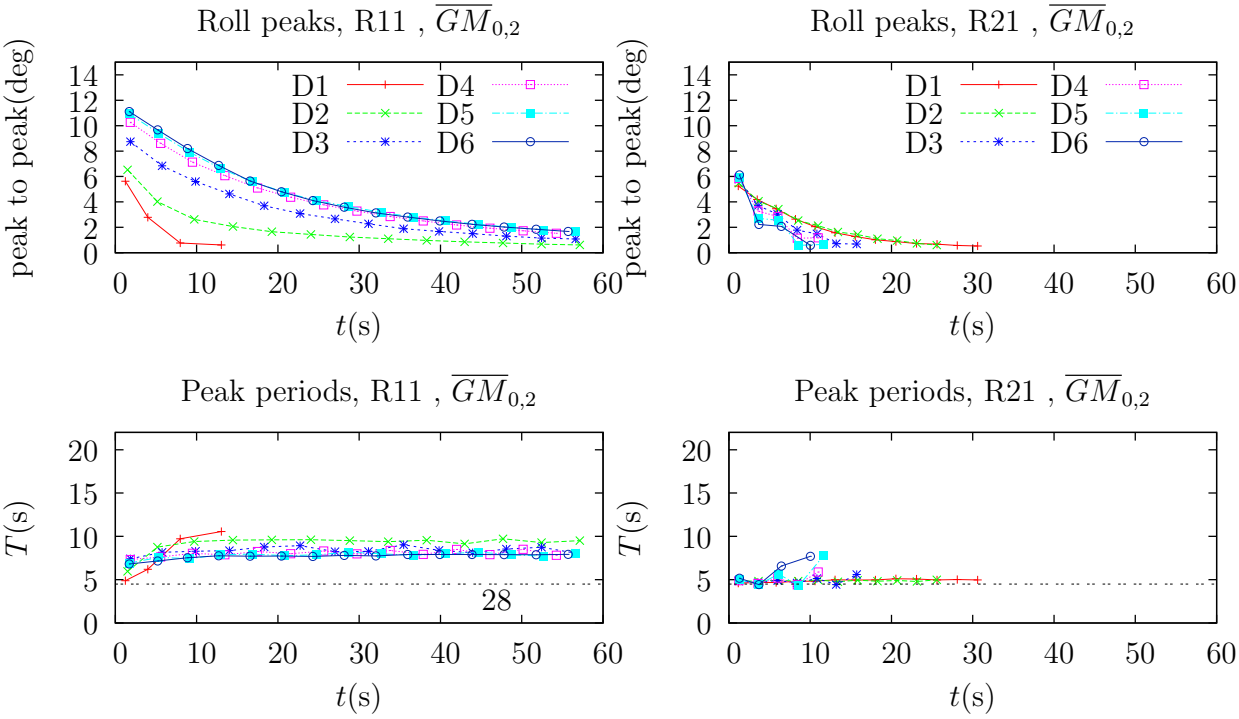

(b) Compartment R11. Higher initial stability $\overline{GM}_{0,2}$.

(d) Compartment R21. Higher initial stability $\overline{GM}_{0,2}$.

Figure 10: Peak to peak roll angles and periods at roll decay tests with constant amount of flooded water in compartment.

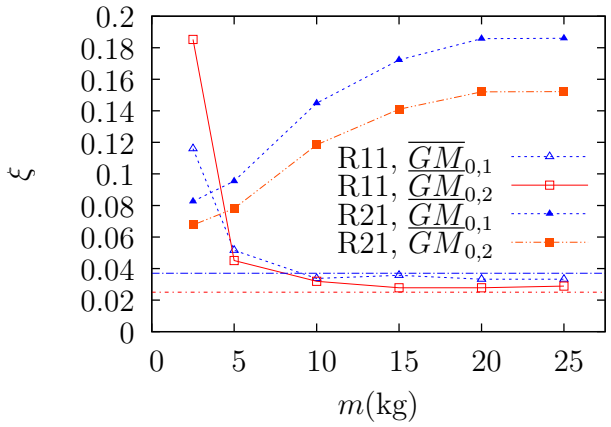

Figure 11: Roll damping ratios for tested compartments and initial stabilities as a funciton of the amount of water in the compartment.

3.3. Transient flooding tests

Damage opening tests were repeated six times for both compartments R11 and R21 and for both initial stabilities. Time histories of the measured roll angle, the increase in draft and the measured water height in the compartments are plotted in Figure 12 - 14. Damage is opened at time $t = 0$. Measured signals are presented without filtering for all six repetitions of the tests. The draft increase is calculated from measured Z_t, *phi* and θ signals according to Equation 1 and therefore contains more noise.

For the tests of flooding to the compartment R11 the barge experiences initially a small, approximately half degree, roll angle to the damage side on starboard (Figure 12). Consequently a bigger transient roll angle is experienced to the portside, opposite to the damage. The first roll angle to the opposite side of the damage at R11, $\overline{GM}_{0,1}$ is -5.4 deg at time 5.5 s after damage. The maximum roll angle at this case is 8.3 deg to the damage side

after two rolls on the opposite side. At higher initial stability (R11, $\overline{GM}_{0,2}$) the first roll angle to the opposite side is 4.0 deg at time 4.1 s after damage, which is the biggest roll angle experienced in this case.

The roll angle to the opposite side causes the lower part of the damage opening to rise above the still water surface and the inflow is stopped for a short time instance around 4 seconds after damage initiation for both initial stabilities. Inflooding water causes the draft to increase. In the draft time history (Figure 13) the cease in the inflooding can be observed. At lower initial stability the inflooding is nearly stopped the second time around 15 seconds where the second roll to the opposite side takes place.

Measured water height on the damage side (Figure 14) initially rises but then starts to lower. At around 4 seconds there is a small peak in the water height. Up until the peak the measured water height at both initial stabilities is almost equal.

Video frame captures in the compartment for the initial stages of flooding are shown in Figure 15 and 16. Surface tracking on the back wall of the compartment has been applied to the tests with compartment R11. The tracked surface is shown in Figure 15. In damage opening tests for compartment R11 the water rushes over the breadth of the compartment to the opposite side. The roll angle turns negative at both initial stabilities around 2.5 seconds after damage initiation. Observing the frame captures of the video recordings in Figure 15 it can be seen that at time $t = 2.0$ s after damage the flooded water is pushed to the opposite side of the damage (portside). The roll angle at this time instant is still on the damage side (starboard).

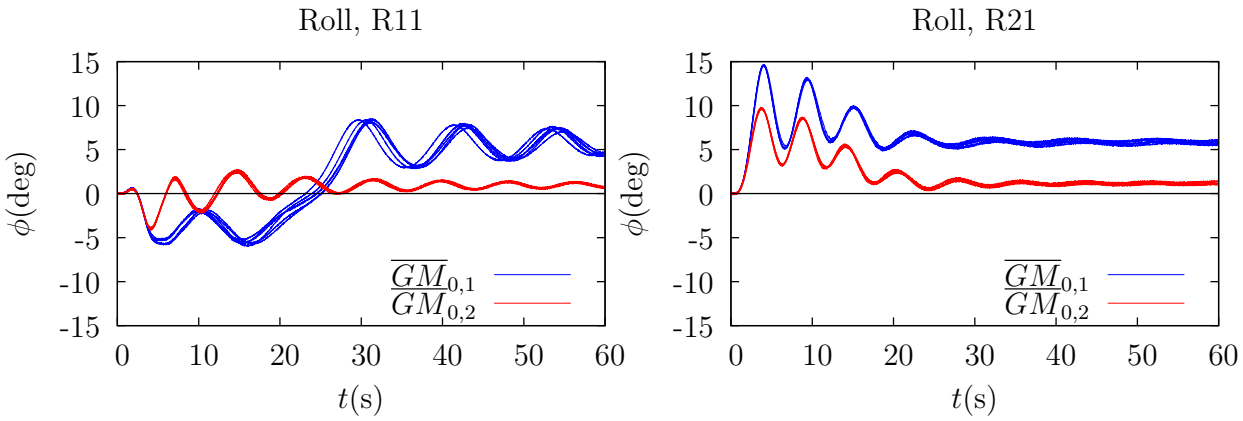

Figure 12: Roll angle for damage opening. Six repeated tests for all cases.

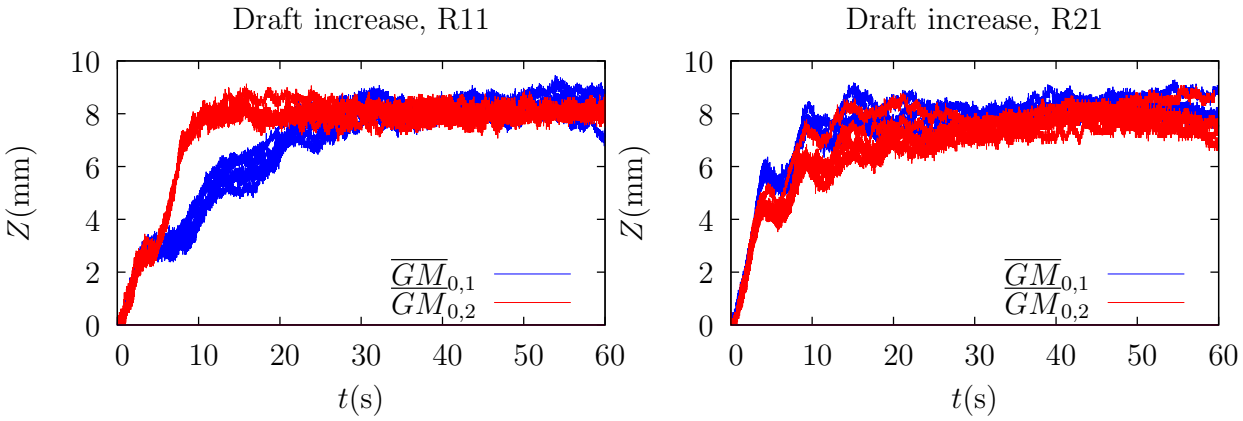

Figure 13: Draft increase for damage opening. Six repeated tests for all cases (except for case: R21 $\overline{GM}_{0,1}$ four repeated tests are shown).

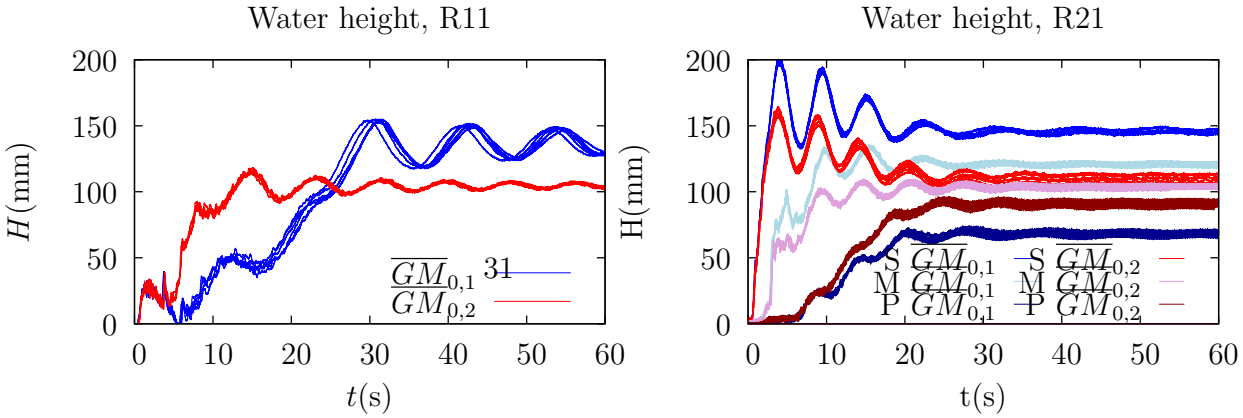

Figure 14: Water height at wave probes in compartment R11 (on left) and in rooms R21S, R21 and R21P (on right) marked respectively by S, M and P in the legend. Six repeated

The position of the flooded water center of gravity *cog* is estimated from the tracked surface. The transversal y-coordinate of the *cog* is shown in Figure 17a for the first 25 seconds together with the roll angle. At the beginning of the flooding the position is on the starboard side, close to the opening. After the first second, the *cog* of the floodwater has moved to the opposite side of the compartment. The roll angle follows. After initial roll angles the flooded water *cog* follows the roll angle. The initial flow to the opposite side plays an important role on the roll response. During the first four seconds of the flooding the response is very similar for both initial stabilities. After that, at the higher initial stability case, the restoring moment rolls the barge back to the starboard. For the lower initial stability the remaining restoring moment is close to zero.

At flooding tests with the divided compartment R21 the initial roll angle is on the damage side. Water flow, cross-flooding, to the opposite side is slowed down by the longitudinal bulkheads with openings. For $\overline{GM}_{0,1}$ the initial and largest roll angle is 14.7 deg at time 4.0 s after damage and for $\overline{GM}_{0,2}$ 9.6 deg at time 3.8 s after damage. The consequence of the asymmetric flooding to the roll response at intermediate stages is important in these cases. Roll time histories are qualitatively similar for damage in compartment R21 at both initial stabilities (Figure 12).

The increase in the draft at damage opening to compartment R21 is faster at the beginning of flooding than for the damage in compartment R11. Roll angle to the damage side increases the inflooding. The draft time history suggests that after the first maximum roll angle some outflooding takes place around 7 seconds time after damage initiation. The outflooding,

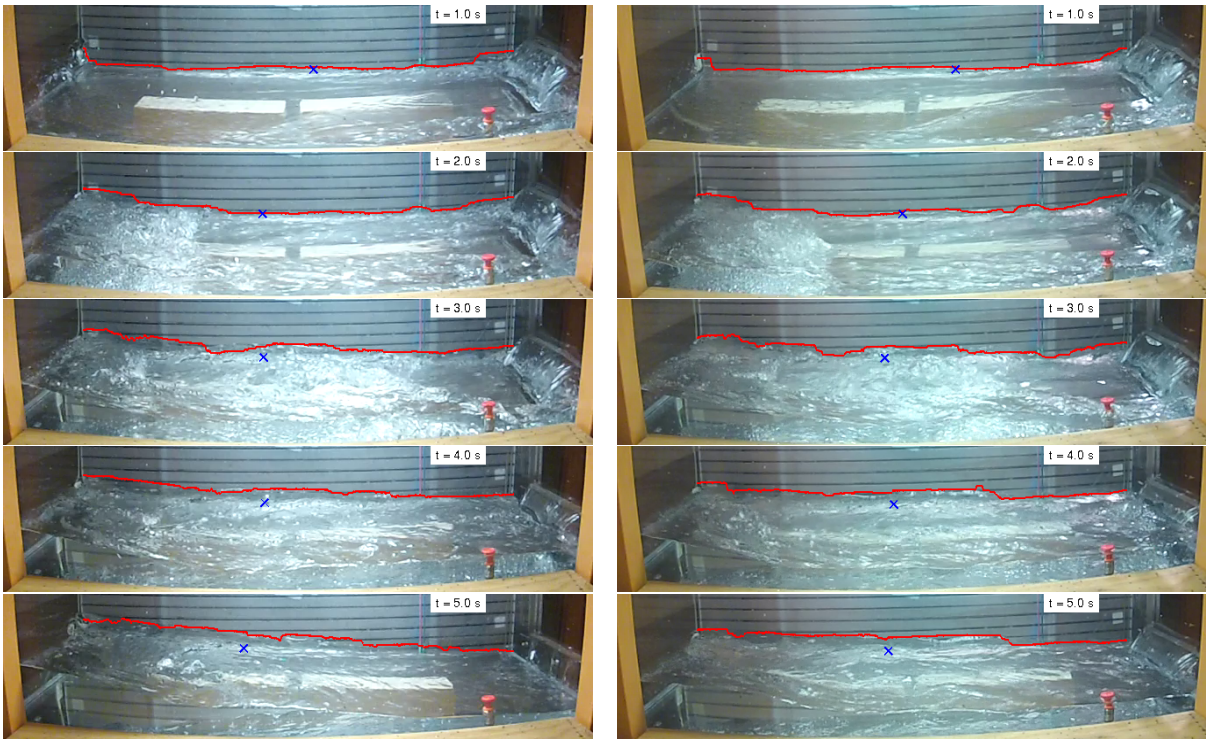

Figure 15: Video capture and tracked water surface at back wall of the flooding test of compartment R11 with $\overline{GM}_{0,1}$ (on left) and with $\overline{GM}_{0,2}$ (on right) at time 1.0,...,5.0 s. Blue $\times$ is showing the estimated position of flooded water *cog* projected to the back wall.

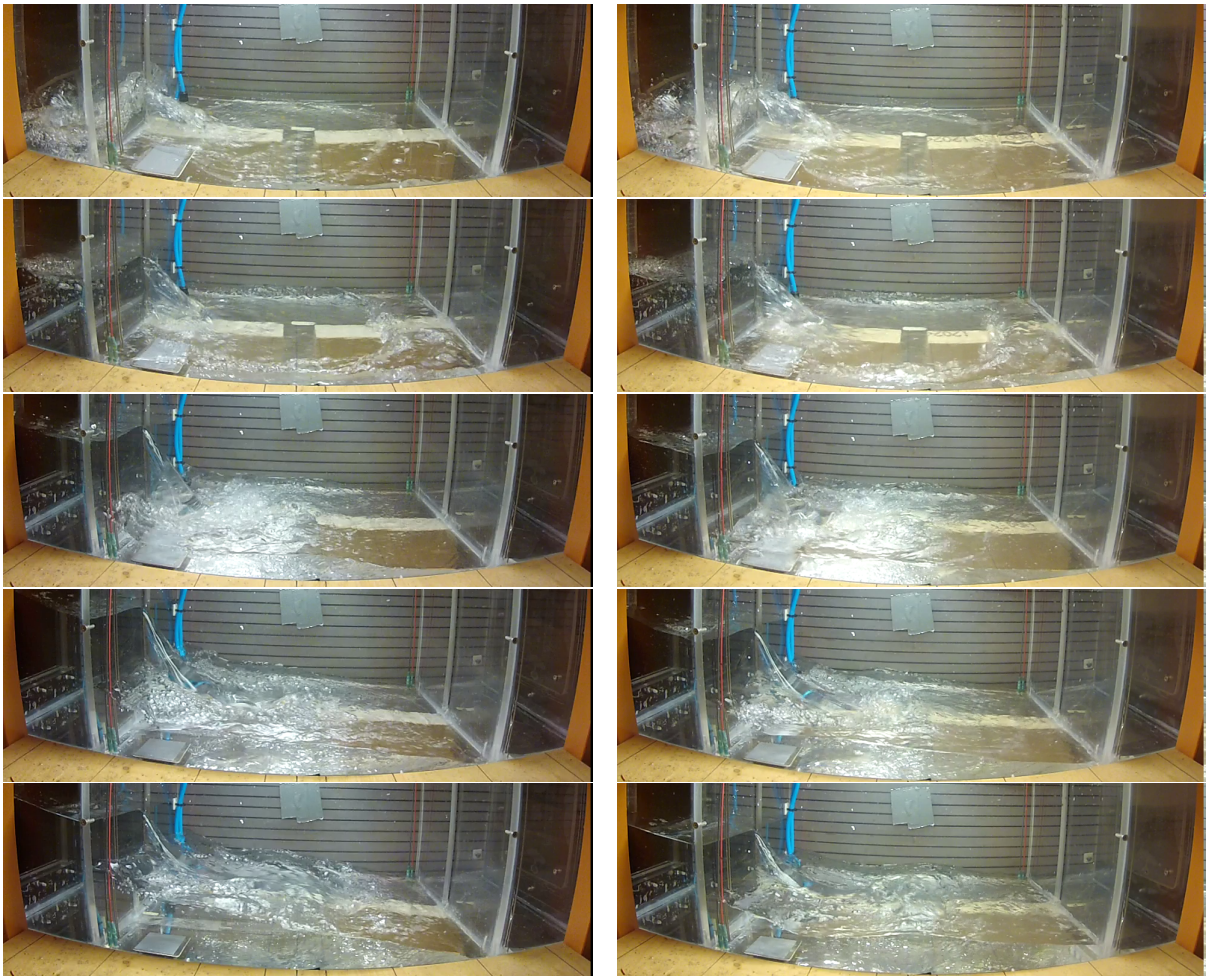

Figure 16: Video capture of the flooding test of compartment R21 with $\overline{GM}_{0,1}$ (on left) and with $\overline{GM}_{0,2}$ (on right) at time 1.0,...,5.0 s.

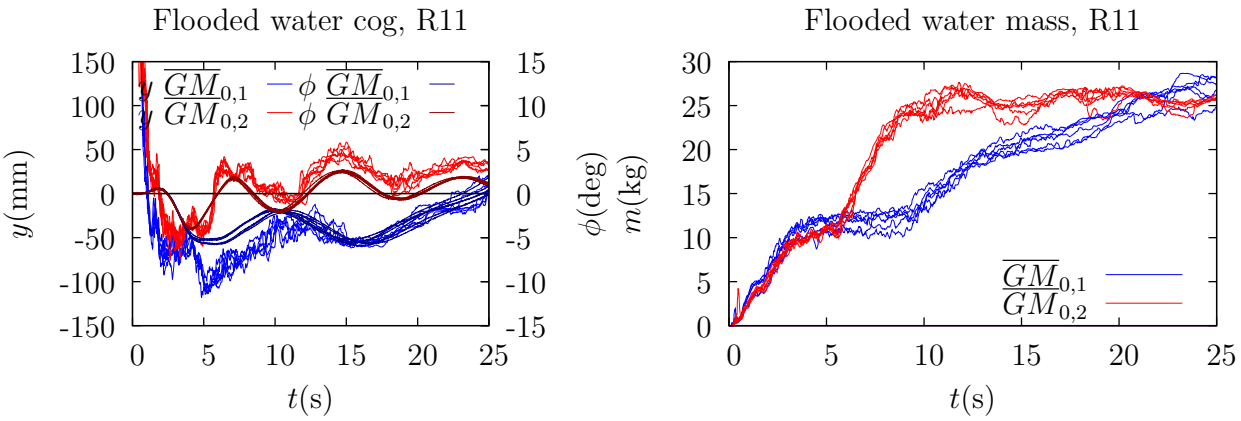

(a) Estimated y-coordinate of flooded water *cog* and measured roll angle of the model.

(b) Flooded water mass estimated from the tracked surface.

Figure 17: Results estimated from the tracked surface.

or the reduction in draft, is again repeated after the second maximum roll angle (Figure 13).

Measurements of the water heights in the compartment R21 (Figure 14) show that the water level on the damage side R21S rises high during the first roll period. The water level in the middle room takes two roll periods to rise. Comparing the time histories of the water heights at different initial stabilities shows that the behaviour is qualitatively similar. The roll angles for divided compartment R21 are larger and dampen faster than for the undivided compartment R11 (Figure 12). The final draft increase is the same (within the measurement precision) for all cases (Figure 13).

4. Discussion

The impact of the floodwater on the roll damping and the transient flooding process are discussed separately in the following subchapters. The impact of the compartment layout was noted to be important for both damping and the actual roll response on the abrupt flooding. A simplified physical model was used in these tests. The model had squared shape with planar surfaces. Compartments were prismatic tanks and the openings rectangular. This enables accurate reproduction of the test setup for the validation purposes. Regardless of the simplified form of hull, its main dimensions corresponding to a typical passenger ship. The only difference being somewhat shorter length. However the studied cases mainly have movements in the roll direction, so the difference in the length is not considered important. The compartment size proportions are quite realistic in terms of the length and width.

4.1. Roll damping

Roll decay tests with constant amount of flooded water show that the rolling decays faster for the damaged divided compartment than for the intact ship, as noted in Lee et al. (2012). The roll was damped fast for the undivided compartment R11 at the smallest amount of water. The natural period of the sloshing estimated by the linear potential theory for the smallest fill height is close to the intact barge roll natural period, for which the water in the compartment acts like an anti-rolling tank. However, roll angles were large enough so that the small amount of water does not totally cover the compartment bottom at all times. Thus the estimated natural sloshing

frequency can vary from the actual one. Viscous effects at the bottom of the tank are more pronounced at low amounts of water. When floodwater meets the wall some run-up against the wall takes place and vortices are formed. Bouscasse et al. (2014b) concluded, in their experimental study, that the dissipation of energy in a coupled roll motion and sloshing system is mostly attributed to the wave breaking. When the amount of water is increased, the water plane is nearly a horizontal plane and less disturbed behaviour of the surface is observed. At larger amounts of floodwater for the undivided compartment the estimated damping ratio was close to the intact barge damping ratio.

Conversely, for the divided compartment R21, the damping increased when the floodwater amount was increased. Roll motion was damped more efficiently in the divided compartment than in the undivided one, except for the smallest fill amount. In the experiments of Armenio et al. (1996a,b) the baffled tank was noted to dampen the roll more efficiently than the unbaffled one. The water surface remained nearly horizontal at all tests for the undivided compartment. The flow through the openings seems to slow down the equalising of the water surface between the openings and thus seems to contribute to the damping. Also the flow through the openings causes energy losses.

The roll period of an intact ship is dependent on the restoring moment and the inertia. For the flooded case the static restoring moment (GZ-curve Figure 3 and 4) steepness changes considerably and its values are even negative or close to zero at a wide range of heel angles for the low initial stability $\overline{GM}_{0,1}$. The roll periods of the flooded undivided compartment are

nearly doubled with respect to the intact model Figure 10. While for the divided compartment the roll periods in flooded condition are nearly the same as for the intact model. The static restoring moments (GZ-curves) are nearly the same for both compartments at the same amounts of water. The slope of the GZ-curve around the equilibrium position for lower initial stability is steeper for the flooded water masses of 2.5 and 5.0 kgs than for larger amounts of flooded water. Thus the actual $\overline{GM}$ value with the water in the compartment is larger for the smaller amounts of water. At these amounts (2.5 and 5.0 kgs) of flooded water the roll period is shorter for compartment undivided compartment (Figure 10a). The slope of the GZ-curve is nearly the same for all masses around the equilibrium position for higher initial stability. Nearly half as steep as for the intact ship. The roll periods at all masses for higher initial stability are nearly doubled. Water motion in the divided compartment is significantly limited in comparison with the undivided compartment due to the longitudinal bulkheads. The total restoring moment estimated by the static heel angle is not necessarily applicable in the dynamic roll motion in a flooded case. Lee et al. (2012) suggested that the increased roll period might be due to the reduction of the total restoring moment by the floodwater. According to the results of this paper it can not be generalized to all flooding conditions.

4.2. Transient flooding

The experiments showed different transient roll response for undivided and divided compartment flooding. The damage, compartment and initial stabilities were the same for both undivided and divided compartment flooding cases. Final equilibrium position is the same for both compartment

layouts. In the transient stage the undivided compartment experienced roll on the opposite side of the damage while for the divided compartment flooding the roll occurred only on the damage side. The transient roll angles being nearly twofold in the divided compartment flooding compared to the undivided compartment. This result has been observed also in the previous studies. The asymmetric flooding has been identified as potentially hazardous to the ship stability (Spouge, 1985; Vredeveldt and Journée, 1991; Santos et al., 2002). International Maritime Organization IMO rules require cross-flooding ducts to enable the floodwater to spread out evenly. In this experimental study, the layouts presented the extreme cases of the compartment with obstructions, one being totally free of all the obstructions and the other with highly restrictive obstructions (walls with narrow openings). In a real ship the compartments would have different obstructions e.g. motor blocks.

However, the study provides a good validation case for the codes predicting the transient roll response to an abrupt flooding. The two presented compartment layout cases being of the two extremities in terms of obstructions point out the importance of the different phenomena; the inflooding jet playing an important role in the undivided compartment case, dynamic water movements in the compartment, the flow to the opposite side, water run-up on the opposite wall and the possible viscous effect at the bottom of the compartment. All of which are highly coupled with the response of the ship, mainly roll motion in the presented cases. The heeling moment due to the flooded water weight at a location away from the center line has an important contribution on the roll response. Of which the water jet seems

to be playing the most important role in case of the undivided compartment, while for the divided compartment the jet is stopped by the dividing non-watertight wall.

Further effects, which were not covered in the presented experiments, are the possible scale effect and the air compression. Of which the the latter has been demonstrated to have an important effect on the progression of flooding (Palazzi and de Kat, 2004; Ruponen et al., 2013). This could be important in the divided compartment case. If full ventilation had not been arranged to the rooms in the divided compartment the air could have been trapped in the compartment and this could have had an effect on the inflooding. The experiments have been simplified in order to concentrate on the coupling of the inflow, floodwater and ship motions. In the future work it would be interesting to perform a systematic study on the effect of the damage size, internal opening sizes and the obstructions on the roll response.

5. Conclusions

The conducted model tests provide valuable validation data for simulation tools assessing damage ship stability and the response in the damage case. Results also provide information on the inflooding water behaviour and quantitative values on impact of compartment layout and initial stability on the flooding and roll response. The flooding process in the transient stage of an abrupt flooding has been carefully measured. The transfer of the flooded water to the opposite side of the damage has been measured with the surface tracking method. This method provides the quantitative data of the water inflooding process. Compared with the conventional water height measure-

ment at one point this method provides the water heights at the total breadth of the compartment. Flooded water volume and the position of its center of gravity were estimated from the tracked surface. This information is useful in the development of numerical simulation tools and can be used for their validation. The presented study confirms and provides further insight into some of the findings of the previous studies. These main findings are listed below.

The quantitative values of the roll damping of the damaged ship have been evaluated. A clear difference in the roll behaviour between the flooded undivided compartment and flooded divided compartment has been observed. When the undivided compartment is flooded the damping is the highest at low amounts of flooded water, when the natural sloshing period is closest to the resonance with the intact ship natural roll period. The evaluated damping ratio is three to six times bigger than for the intact ship. At higher amounts of floodwater, the sloshing periods of are substantially lower compared to the roll period. The evaluated damping ratio at higher fill amounts is close to the intact ship damping ratio. For the divided compartment, the damping is the smallest at the lowest fill amounts and increases with increasing fill amount. At all fill amounts, the damping is higher for the flooded ship than for the intact one. Natural sloshing periods are substantially lower in comparison with the intact ship roll period at all fill amounts for the divided compartment. The flow through the internal openings contributes to the damping.

The roll response of the model at an abrupt flooding when the opening is relatively large depends largely on the internal arrangement of the flooded

compartment. For the undivided compartment, the flooded water flows to the opposite side of the compartment and causes roll to the opposite side. Due to this roll angle the damage opening is lifted and the inflow is reduced or even stopped. Difference in the initial stability can lead to quantitatively different roll response when the undivided compartment is flooded. For the divided compartment, the cross flooding is slowed down by the obstructions or non-watertight openings. The initial roll occurs to the damage side and thus accelerates the inflooding and further slows down the cross flooding. Initial roll to the damage side can be relatively high. For the tested model and opening, the highest roll angle with the divided compartment is nearly threefold in compared to the undivided compartment. For divided compartment higher initial stability mainly moderates the roll response angles.

Besides of the increased damping and increased roll periods, the overall roll behaviour of the flooded ship has been observed to change drastically from the intact one. Floodwater adds mass and inertia to the ship. Through free floodwater surface the mass is free to deform itself and no fixed location nor inertia values can be assigned to it. When predicting the motions of a damaged ship condition, it cannot be treated as a rigid body with constant inertia and damping properties, but rather as a system with changing inertia or a system with more than six degrees of freedom, where the mass of the floodwater can vary in time. These observations provide important instruction on the further development of numerical models for damaged ship motions.

The following experimental studies can be recommended for potential future work. In order to assign the damping due to the exchange of the water

between sea and the compartment, roll decay tests for damaged ship with damage open to the sea should be performed. In this work the impact of the compartment layout on the flooding response has been studied for undivided and divided compartments. It could be beneficial to perform tests by varying the internal opening size, in order to cover the area between the divided and undivided compartments. Furthermore, the abrupt flooding tests with different initial heel conditions could provide data on the initial impact due to collision or grounding on the transient flooding process. Additionally, the tests in waves with damage initiated at varying roll angles could be performed. However the experimental campaign could become quite extensive.

Acknowledgements

The authors would like to express their gratitude to the Aalto University Marine Technology Towing Tank technicians Teemu Päivärinta and Pentti Tukia for their indispensable help in arranging the tests. The research presented was carried out as a part of Fimeccs research program Innovations and Network and was funded by Tekes. Financial funding is greatly appreciated.

References

Armenio, V., Francescutto, A., Rocca, M. L., 1996a. On the roll motion of a ship partially filled unbaffled and baffled tanks. Part I. Mathematical model and experimental setup. Internatinal Journal of Offshore and Polar Engineering 6 (4), 278–283.

Armenio, V., Francescutto, A., Rocca, M. L., 1996b. On the roll motion of a ship partially filled unbaffled and baffled tanks. Part II. Numerical and

experimental analysis. Internatinal Journal of Offshore and Polar Engineering 6 (4), 283–290.

Begovic, E., Mortola, G., Incecik, A., Day, A., 2013. Experimental assessment of intact and damaged ship motions in head, beam and quartering seas. Ocean Engineering 72 (0), 209 – 226.

Bouscasse, B., Colagrossi, A., Souto-Iglesias, A., Cercos-Pita, J. L., 2014a. Mechanical energy dissipation induced by sloshing and wave breaking in a fully coupled angular motion system. I. Theoretical formulation and numerical investigation. Physics of Fluids 26 (3).
URL http://scitation.aip.org/content/aip/journal/pof2/26/3/10.1063/1.4869233

Bouscasse, B., Colagrossi, A., Souto-Iglesias, A., Cercos-Pita, J. L., 2014b. Mechanical energy dissipation induced by sloshing and wave breaking in a fully coupled angular motion system. II. Experimental investigation. Physics of Fluids 26 (3).
URL http://scitation.aip.org/content/aip/journal/pof2/26/3/10.1063/1.4869234

Chan, H.-S., Atlar, M., Incecik, A., 2002. Large-amplitude motion responses of a roro ship to regular oblique waves in intact and damaged conditions. Journal of Marine Science and Technology 7 (2), 91–99.
URL http://dx.doi.org/10.1007/s007730200017

de Kat, J. O., 2000. Dynamics of a ship with partially flooded compartment.

In: Vassalos, D., Hamamoto, M., Papanikolaou, A., Molyneux, D. (Eds.), Contemporary Ideas on Ship Stability. Elsevier Science, pp. 249–263.

de Kat, J. O., van't Veer, R., September 2001. Mechanisms and physics leading to the capsize of damaged ships. In: Proceedings of the 5th International Ship Stability Workshop. Trieste, Italy.

Faltinsen, O. M., Timokha, A. N., 2009. Sloshing. Cambridge University Press, New York.

Goerlandt, F., Kujala, P., 2014. On the reliability and validity of shipship collision risk analysis in light of different perspectives on risk. Safety Science 62 (0), 348 – 365.
URL http://www.sciencedirect.com/science/article/pii/S0925753513002191

Goerlandt, F., Montewka, J., Kujala, P., 2014. Tools for an extended risk assessment for ropax ship-ship collision. In: Beer, M., Au, S.-K., Hall, J. W. (Eds.), Vulnerability, Uncertainty, and Risk: Quantification, Mitigation, and Management. American Society of Civil Engineers, Reston, Virginia, pp. 2291 – 2302.

Ikeda, Y., Kamo, T., September 2001. Effects of transient motion in intermediate stages of flooding on the final condition of a damaged PCC. In: Proceedings of the 5th International Ship Stability Workshop. Trieste, Italy.

Ikeda, Y., Ma, Y., February 2000. An experimental study on large roll motion in intermediate stage of flooding due to sudden ingress water. In: Proceed-

ings of the 7th International Conference on Stability of Ships and Ocean Vehicles. Launceston, Tasmania, Australia, pp. 270–285.

Ikeda, Y., Shimoda, S., Takeuchi, Y., September 2003. Experimental studies on transient motion and time to sink of a damaged large passenger ship. In: Proceedings of the 8th International Conference on Stability of Ships and Ocean Vehicles. Madrid, Spain, pp. 243–252.

Journée, J. M. J., September 1997. Liquid cargo and its effect on ship motions. In: 6th International Conference on Stability of Ships and Ocean Vehicles. Vol. 1. Varna, Bulgaria, pp. 137–150.

Journée, J. M. J., Vermeer, H., Vredeveldt, A. W., September 1997. Systematic model experiments on flooding of two ro-ro vessels. In: 6th International Conference on Stability of Ships and Ocean Vehicles. Vol. 2. Varna, Bulgaria, pp. 81–98.

Khaddaj-Mallat, C., Alessandrini, B., Rousset, J.-M., Ferrant, P., 2012. An experimental study on the flooding of a damaged passenger ship. Ships and Offshore Structures 7 (1), 55–71.

Khaddaj-Mallat, C., Rousset, J.-M., Ferrant, P., 2011. The transient and progressive flooding stages of damaged ro-ro vessels: A systematic review of entailed factors. Journal of Offshore Mechanics and Arctic Engineering 133 (3).

Korkut, E., Atlar, M., Incecik, A., 2004. An experimental study of motion behaviour with an intact and damaged ro-ro ship model. Ocean Engineering 31 (3-4), 483–512.

Lamb, H., 1945. Hydrodynamics, sixth Edition. Dover Publications.

Lee, D., Hong, S., Lee, G.-J., 2007. Theoretical and experimental study on dynamic behavior of a damaged ship in waves. Ocean Engineering (34), 21–31.

Lee, S., You, J.-M., Lee, H.-H., Lim, T., Rhee, S. H., Rhee, K.-P., 2012. Preliminary tests of a damaged ship for CFD validation. International Journal of Naval Architecture and Ocean Engineering 4 (2), 172–181.

Levander, K., 2003-2004. Passenger ships. In: Lamb, T. (Ed.), Ship design & construction. Vol. II. Society of Naval Architects and Marine Engineers, Jersey City, NJ.

Lobovský, L., Botia-Vera, E., Castellana, F., Mas-Soler, J., Souto-Iglesias, A., 2014. Experimental investigation of dynamic pressure loads during dam break. Journal of Fluids and Structures 48 (0), 407 – 434.
URL http://www.sciencedirect.com/science/article/pii/S0889974614000656

Macfarlane, G. J., Renilson, M. R., Turner, T., 2010. The transient effects of flood water on a warship in calm water immediately following damage. Transactions RINA, International Journal of Maritime Engineering 152, part A4.

Manderbacka, T., Kulovesi, J., M. A. Celis C., Matusiak, J. E., Neves, M. A. S., July 2014. Model tests on the impact of the opening location on the water motions in a flooded tank with two compartments. Ocean Engineering 84, 67–80.

URL http://www.sciencedirect.com/science/article/pii/S0029801814001346

Montewka, J., Ehlers, S., Goerlandt, F., Hinz, T., Tabri, K., Kujala, P., 2014. A framework for risk assessment for maritime transportation systemsa case study for open sea collisions involving ropax vessels. Reliability Engineering & System Safety 124 (0), 142 – 157.
URL http://www.sciencedirect.com/science/article/pii/S0951832013003116

Napa Ltd, Aalto University, 2013. Aalto University & NAPA: Flooding model test for ITTC benchmark study (ITTC-Box).
URL http://shipstab.org/index.php/data-access/list-of-available-benchmarking-data/30-ittc-box-aalto-napa

Palazzi, L., de Kat, J., January 2004. Model experiments and simulations of a damaged ship with air-flow taken into account. Marine Technology 41 (1), 38 – 44.

Papanikolaou, A., 2001. Benchmark study on the capsizing of a damaged ro-ro passenger ship in waves. Tech. rep., National Technical University of Athens.

Papanikolaou, A., Spanos, D., November 2004. 24th ITTC Benchmark Study on Numerical Prediction of Damage Ship Stability in Waves - Preliminary Analysis and Results. In: Proceedings of the 7th International Ship Stability Workshop. Shanghai, China.

Ruponen, P., 2006. Model tests for progressive flooding of a box-shaped barge. Tech. rep., Helsinki University of Technology.

Ruponen, P., November 2007. Progressive flooding of a damaged passenger ship. Ph.D. thesis, Helsinki University of Technology, Ship Laboratory.

Ruponen, P., Kurvinen, P., Saisto, I., Harras, J., 2013. Air compression in a flooded tank of a damaged ship. Ocean Engineering 57 (0), 64 – 71.
URL http://www.sciencedirect.com/science/article/pii/S002980181200368X

Ruponen, P., Sundell, T., Larmela, M., 2007. Validation of a simulation method for progressive flooding. International Shipbuilding Progress 54 (4), 305–321.

Santos, T. A., Winkle, I. E., Guedes Soares, C., 2002. Time domain modelling of the transient asymmetric flooding of ro-ro ships. Ocean Engineering 29 (6), 667–688.

Spouge, J. R., 1985. The Technical Investigation of the Sinking of the Ro-Ro Ferry European Gateway. Transactions of RINA 127, 49–72.

Ståhlberg, K., Goerlandt, F., Ehlers, S., Kujala, P., 2013. Impact scenario models for probabilistic risk-based design for shipship collision. Marine Structures 33 (0), 238 – 264.
URL http://www.sciencedirect.com/science/article/pii/S095183391300049X

van Walree, F., Papanikolaou, A., August 2007. Benchmark study of numerical codes for the prediction of time to flood of ships: Phase i. In:

Proceedings of the 9th International Ship Stability Workshop. Hamburg, Germany.

van't Veer, R., de Kat, J. O., February 2000. Experimental and numerical investigation on progressive flooding and in complex compartment geometries. In: Proceedings of the 7th International Conference on Stability of Ships and Ocean Vehicles. Launceston, Tasmania, Australia, pp. 305–321.

van't Veer, R., Peters, W., Rimpelä, A.-L., de Kat, J., November 2004. Exploring the influence of different arrangements of semi-watertight spaces on survivability of a damaged large passenger ship. In: Proceedings of the 7th International Ship Stability Workshop. Shanghai, China.

Vassalos, D., Ikeda, Y., Jasionowski, A., Kuroda, T., November 2004. Transient flooding on large passenger ships. In: Proceedings of the 7th International Ship Stability Workshop. Shanghai, China.

Vredeveldt, A. W., Journée, J. M. J., April 1991. Roll motions of ships due to sudden water ingress, calculations and experiments. In: RINA'91, International Conference on Ro-Ro Safety and Vulnerability the Way Ahead. London, England.

Zhao, W., Yang, J., Hu, Z., Tao, L., 2014. Coupled analysis of nonlinear sloshing and ship motions. Applied Ocean Research 47 (0), 85 – 97.
URL http://www.sciencedirect.com/science/article/pii/S0141118714000388